MTL TR 91-31
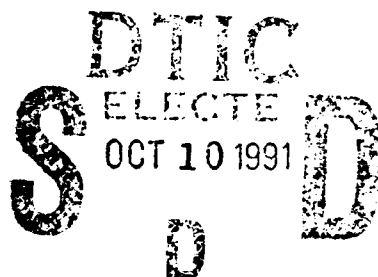
METALLURGICAL AND MECHANICAL ANALYSES OF A FAILED FUSE HOLDER FROM THE XM264 ROCKET

WEGO WANG, JOHN C. BECK, and MARTIN G. H. WELLS
METALS RESEARCH BRANCH

DTIC
ELECTE
OCT 10 1991
S
D

August 1991

91-12819

‖‖‖‖‖‖‖‖‖‖‖‖

US ARMY
LABORATORY COMMAND
MATERIALS TECHNOLOGY LABORATORY

U.S. ARMY MATERIALS TECHNOLOGY LABORATORY
Watertown, Massachusetts 02172-0001

REPORT DOCUMENTATION PAGE		READ INSTRUCTIONS BEFORE COMPLETING FORM
1. REPORT NUMBER MTL TR 91-31	2. GOVT ACCESSION NO.	3. RECIPIENT'S CATALOG NUMBER
4. TITLE *(and Subtitle)* METALLURGICAL AND MECHANICAL ANALYSES OF A FAILED FUSE HOLDER FROM THE XM264 ROCKET		5 TYPE OF REPORT & PERIOD COVERED Final Report
		6 PERFORMING ORG. REPORT NUMBER
7. AUTHOR(s) Wego Wang, John C. Beck, and Martin G. H. Wells		8. CONTRACT OR GRANT NUMBER(s)
9. PERFORMING ORGANIZATION NAME AND ADDRESS U.S. Army Materials Technology Laboratory Watertown, Massachusetts 02172-0001 ATTN: SLCMT-EMM		10. PROGRAM ELEMENT, PROJECT, TASK AREA & WORK UNIT NUMBERS
11. CONTROLLING OFFICE NAME AND ADDRESS U.S. Army Laboratory Command 2800 Powder Mill Road Adelphi, Maryland 20783-1145		12 REPORT DATE August 1991
		13. NUMBER OF PAGES 25
14. MONITORING AGENCY NAME & ADDRESS(if different from Controlling Office)		15. SECURITY CLASS. (of this report) Unclassified
		15a. DECLASSIFICATION/DOWNGRADING SCHEDULE

16. DISTRIBUTION STATEMENT *(of this Report)*

Approved for public release; distribution unlimited.

17. DISTRIBUTION STATEMENT *(of the abstract entered in Block 20, if different from Report)*

18. SUPPLEMENTARY NOTES

19. KEY WORDS *(Continue on reverse side if necessary and identify by block number)*

Aluminum alloys	Fuse holders	Metallurgical analysis
Die casting	Explosive pressure	
Radiography	Failure analysis	

20. ABSTRACT *(Continue on reverse side if necessary and identify by block number)*

(SEE REVERSE SIDE)

DD FORM 1473 JAN 73 EDITION OF 1 NOV 65 IS OBSOLETE

Block No. 20

ABSTRACT

One aluminum fuse holder from the XM264 red phosphorus smoke rocket that failed during testing was analyzed to determine the cause of failure. Cracks were observed on both sides of the die cast fuse holder. Radiographic analysis was conducted to confirm the damage observed. All the dimensions of this failed fuse holder were found to be within the requirements specified in the part drawing, except the central cup. This region was 30% thinner than specified. Metallographic analysis indicated a mixed fine-grained and eutectic structure in the thin center-disc area and a large dendritic structure in the thick circumferential area. Fractographic examination of the fracture surface showed fracture initiating at large brittle impurity-rich particles. A stress analysis concluded that failure occurred as a result of insufficient material thickness in the central cup region and from stress concentration around the wall edge. Suggestions for a new design with thicker central sections were confirmed by U.S. Army Chemical Research, Development and Engineering Center at Aberdeen Proving Ground, Maryland.

CONTENTS

INTRODUCTION

A failed fuse holder from the XM264 rocket was received in May, 1990 for failure analysis at the U.S. Army Materials Technology Laboratory (MTL), Watertown, Massachusetts. It is made of QQ-A-591F (380) aluminum alloy by die casting at Cast Rite Corporation, Gardena, California.

This rocket is used to provide a concealing smoke screen. The rocket warhead consists of an aluminum case, an M439 electronic time fuse, an expulsion charge assembly, 72 smoke pellets made from a red phosphorus composition, 18 felt separators, a base nose cone assembly, and an outer nose cone assembly as shown in Figure 1. The fuse is enclosed by a fuse holder and located in the warhead base. The fuse is detonated at a predetermined time to ignite the expulsion charge. The hot gasses from the burning expulsion charge travel up through the center channel of the pellet stack igniting the pellets. Upon expulsion, the burning pellets disperse and fall to the ground, producing a voluminous cloud of smoke.

To evaluate the performance of the new rocket, static expulsion and out-of-line fuse safety tests were conducted on March 15, 1990. Seven of eight static expulsion warheads had an expulsion with good smoke production. Three of eight out-of-line fuse safety warheads failed the test when the expulsion cup cracked. The testing was halted after the out-of-line fuse safety test showed failures. One failed fuse holder was sent to MTL for analysis.

EVALUATION PROCEDURES

The fuse holder received showed visible cracks on both sides and the following evaluations were performed in chronological order:
> Radiographic Analysis
> Dimension Verification
> Optical Metallography
> Fractographic Examination Using SEM and EDS*
> Macro and Microhardness Tests
> Density and Porosity Evaluation
> Process Evaluation
> Stress Analysis
> * SEM - Scanning Electron Microscopy
> EDS - Energy Dispersive Spectroscopy (X-ray)

Radiographic Analysis

The primary objective of the radiographic analysis was to examine the fuse holder nondestructively to check for internal cracks and irregularities. Two surface cracks were observed on the external side of the fuse holder; however, no evidence of any further damage or fracture was found. Two semi-circular images were observed in the radiograph resulting from the difference in metal thickness. Nevertheless, the examination was not conclusive, perhaps partially due to the fact that the external fuse holder surface was heavily covered with debris as a result of the previous safety test.

Dimension Verification

The dimensions of this failed fuse holder were carefully verified by micrometer measurements. Most measured dimensions were found to be within the requirements specified in the original part drawing. However, the average measured thickness of 5 different locations throughout the center-cup area is only 0.010 inch, that is about 30% less than the nominal required
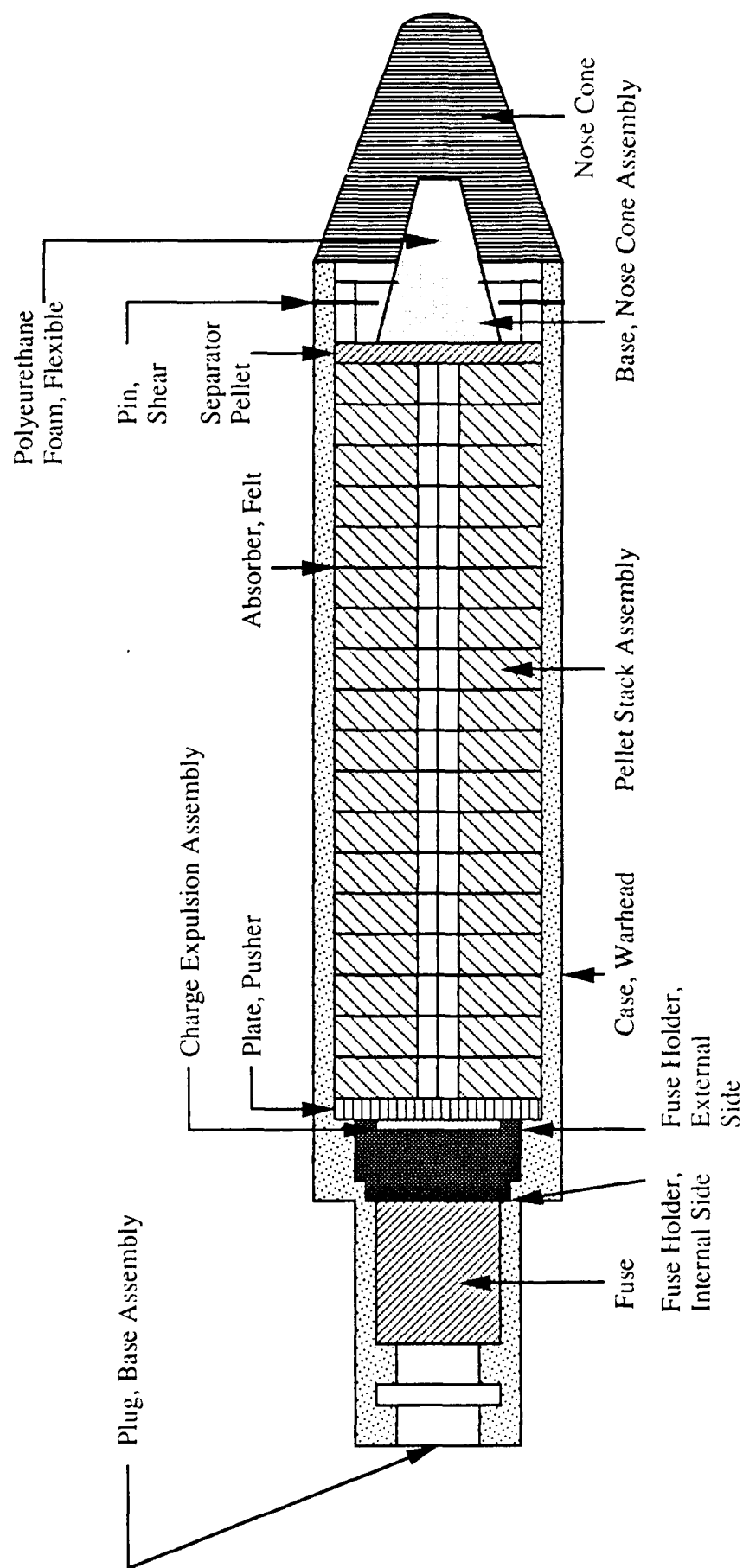
Figure 1. An Overview of the 264 Rocket Warhead

2

thickness (0.015+0.005). The surrounding center-disc thickness is 0.075±0.005 inch in the drawing, compared with an average measured thickness of 0.070 inch, or about 7% thinner than the nominal value specified. It also should be noted that the outermost circumferential surface is oblique by 0.020 inch (i.e. has a taper of 15°) which is not shown in the drawing. The measured dimensions are shown in Figure 2 which illustrates a simplified cross-section front view.

An overall macrograph of the fuse holder casting is shown in Figure 3(a). A large crack located directly underneath the wall edge of the internal side in which the explosive charge firing occurred was observed as shown in Figure 3(b). Two surface cracks were found on the external side as shown in Figures 4 (a) and (b). The dimension measurements indicate that these two cracks are located directly opposite the inner surface recess wall. Several secondary cracks are scattered around the above-mentioned primary cracks. However, no cracks propagated completely through the thickness of the center disc.

From the depth measurement of the center-disc region, there was continuous bending deformation throughout the center-disc with a severe "bump" around the primary crack area and a moderate one in the center-cup area. It should be noted that the center-cup area is vulnerable to potential failure. In Figure 5, small hair-line cracks are observed on the surface of this region. Similar depth measurements were also conducted for an "undamaged" part, where a uniform depth (i.e. undeformed surface) was found.

Materials

The chemical composition of the fuse holder material was analyzed at Metal Analysis, Inc., Huntington, CA. The result is tabulated in Table I. The standard composition of 380 aluminum is also included for comparison.

Table I. MEASURED AND STANDARD CHEMICAL COMPOSITIONS

| Element	Cu	Fe	Mn	Si	Mg	Zn	Ni	Sn	Al
Measured*	3.42	0.69	0.15	8.42	0.01	2.00	0.05	<0.01	Bal.
Standard(1)									
Maximum	4.00	2.00	0.50	9.50	0.10	3.00	0.50	0.35	Bal.
Minimum	3.00	-	-	7.50	-	-	-	-	-

* Courtesy of Cast Rite Corporation, Gardena, CA.

The mechanical properties of 380 aluminum alloy are listed below (1,2)

Tensile strength:	46 ksi (317 MPa)
0.2% offset yield strength:	23 ksi (160 MPa)
Elongation in 2 inches (50 mm):	2.5 to 3.5%
Shear strength:	28 ksi (195 MPa)
Young's modulus:	10.3 x 10^6 psi (71.0 GPa)
Shear modulus:	3.85 x 10^6 psi (26.5 GPa)

---

1   Federal Specification: Aluminum Alloy Die Castings, QQ-A-591F, January 19, 1981.

2   ASM Metals Handbook, p.170, v.2, 9th ed., Metals Park, Ohio, 1979.
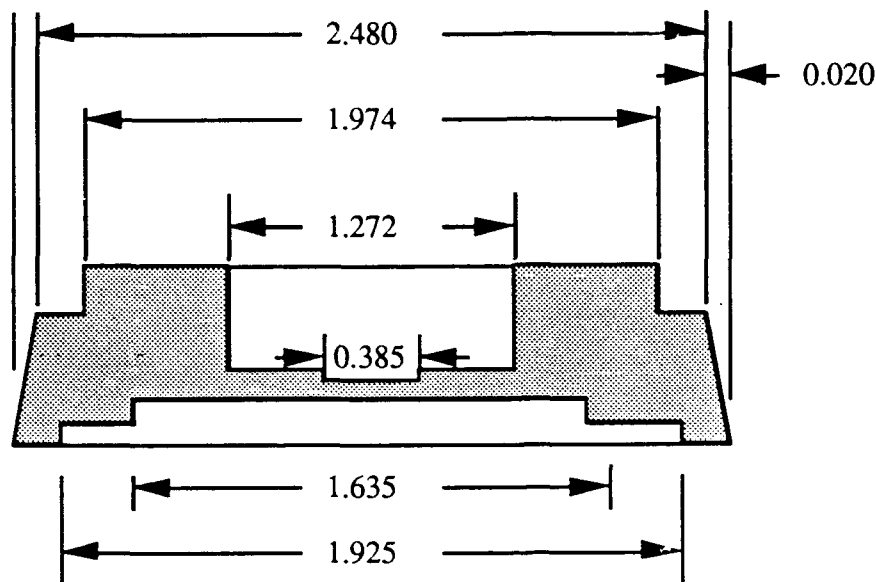
(a) Front view (simplified) with external side downward
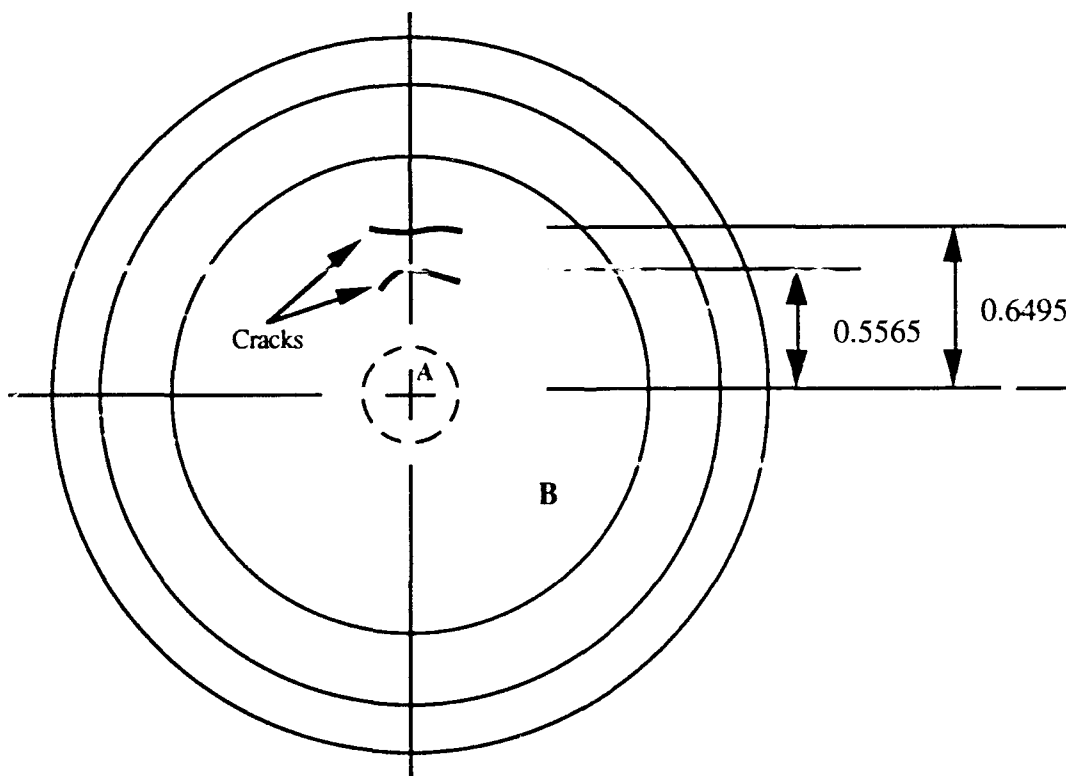
(b) External side view

Figure 2. The measured dimensions of the fuse holder, in inches; A: center cup, specified and measured thicknesses are 0.015+0.005 and 0.010 inch, respectively; and B: center disc, specified and measured thicknesses are 0.075±0.005 and 0.070 inch, respectively.
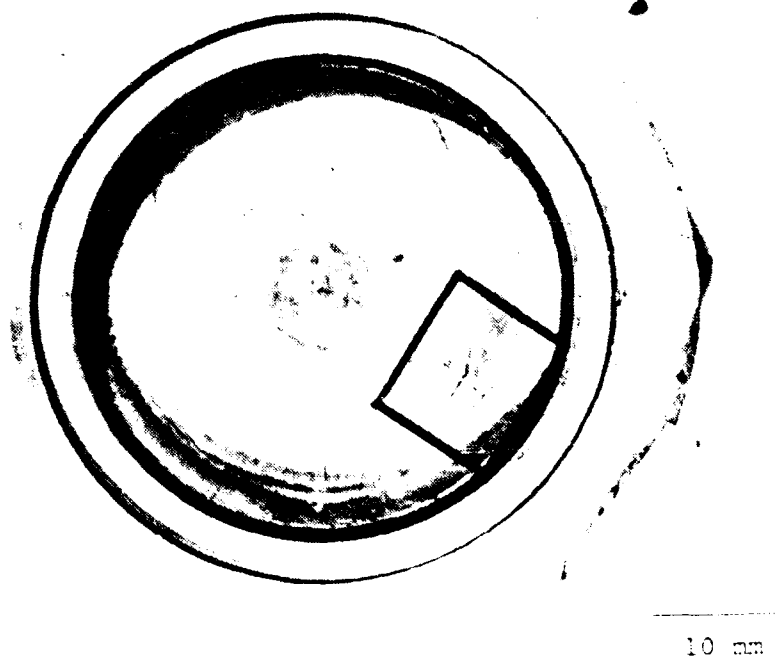
4
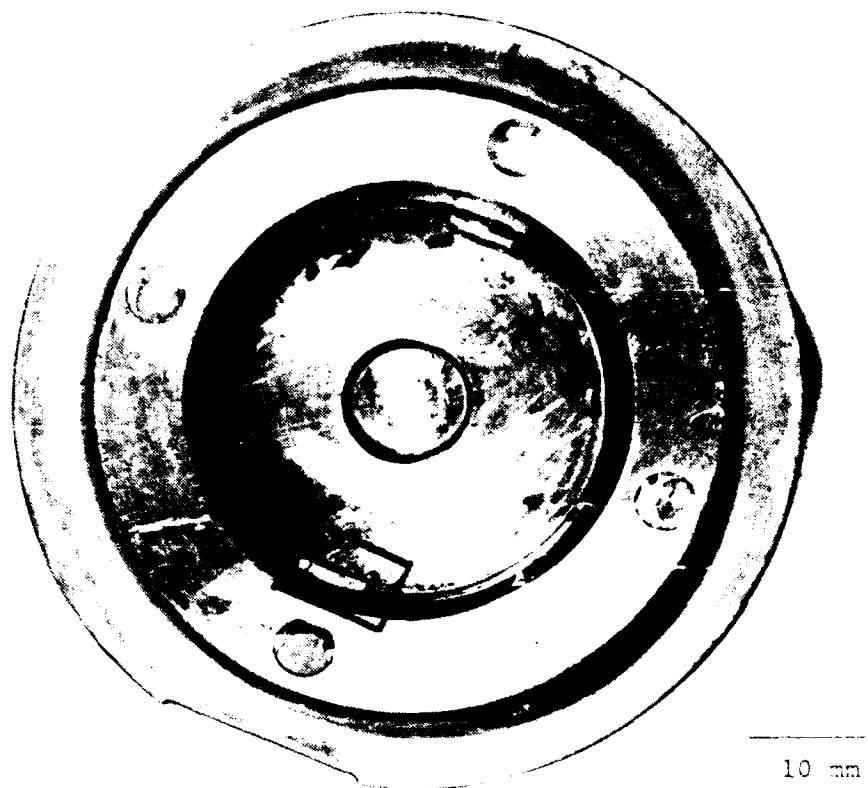
(a) Overview

(b) Close-up view

Figure 3. The internal side of the fuse holder showing a primary crack
directly underneath the wall edge as indicated by the arrow.

(a) Overview

(b) Close-up view

Figure 4. The external side of the fuse holder showing two large cracks.

Figure 5. Optical metallograph showing the early development
of cracks in the center-cup area as indicated by the arrow.

Optical Metallography

As shown in Figure 6, the thin center-disc and the thick bulk areas show two kinds of microstructure. A mixture of primary fine-grained and eutectic microstructures is observed in the center-disc area, with most grains ranging in size from 4 to 10 μm. Fine silicon particles observed in the eutectic structure result from the higher cooling rate in this area. In contrast, the microstructure in the thick bulk area consists of coarse dendrites and a network of acicular interdendritic particles of silicon and $CuAl_2$ due to the slower cooling rate of this area. Several second phases and inclusions are observed throughout both the thin center-disc and the thick circumferential bulk areas. The EDS study of the cross-section and the fracture surface indicates that these phases and/or inclusions are either Cu-, Fe-, Mn-, Pb-rich or residual aluminum. Generally speaking, these particles can initiate cracks if their size is larger than 6 μm in diameter. Composition segregation is also observed with the dendritic cellular structure. There is no evidence of any other severe casting defects.

Fractographic Examination Using SEM and EDS

The specimen was immersed in liquid nitrogen and then forced open to reveal the original crack surface for fractographic examination. These fracture surfaces were carefully examined to identify the crack initiation mechanism and fracture mode. The typical fracture surface with a ductile matrix and cracked brittle particles is shown in Figure 7. No specific crack initiation sites were observed in the matrix, indicating sufficient matrix strength. However, a closer examination at a higher magnification revealed that cracking often starts within brittle impurity particles. A cavity with a diameter of about 20 μm was observed and is shown in the center of Figure 8. The EDS analysis obtained from the center of this region indicated an iron-rich particle. A close-up examination of the bottom of this cavity indicated that a brittle crack was initiated within the iron-rich particle buried in the matrix as shown in Figure 9.

A relatively large (about 150 μm) aluminum particle was observed as shown in Figure 10. This soft aluminum particle did not show any signs of brittle cracking. Though it did not initiate a crack, it did not halt crack propagation. It served as a soft region in the matrix and weakened the overall material strength. Residual aluminum particles should be eliminated by better process control. In addition to this aluminum particle, a few unexpected impurity inclusions and particles were observed as shown in Figure 11. Particles were either Cu-, Mn-, or Fe-rich, respectively. Most second phase particles were very small and presented little direct threat for crack initiation. The observation of a Pb-rich particle, as shown in Figure 12, was unexpected. This Pb-rich particle might come from the explosive charge or other accidental contamination.

Microhardness Tests

Extensive microhardness tests were conducted to detect potential heterogeneities in material strength throughout the sample. This might result from the variations in microstructure from dendritic to fine grained. For microhardness measurement, samples were cut from the center-disc area and the thick circumferential area. Tukon microhardness measurements with a 500 g load were taken at 0.015 inch intervals for each of the twenty-six data point traverses with the results included in Appendix I. The average Knoop microhardness values are 98.3 with a population standard deviation of 3.8, and 89.6 with a population standard deviation of 10.65 for the thin center-disc and the circumferential bulk areas, respectively. Note that the thin center-
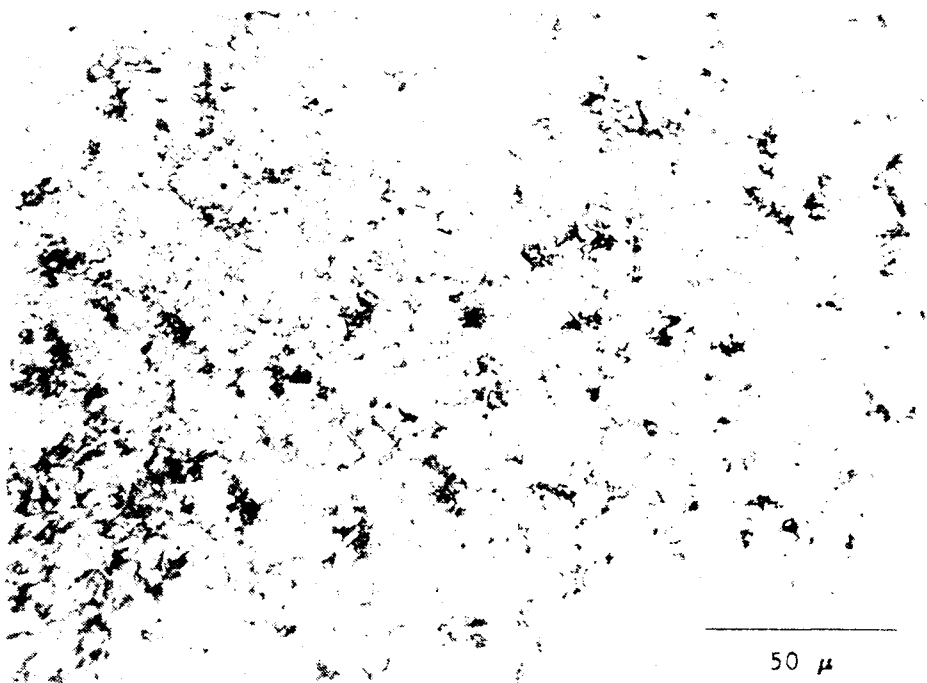
(a) The thin center-disc area
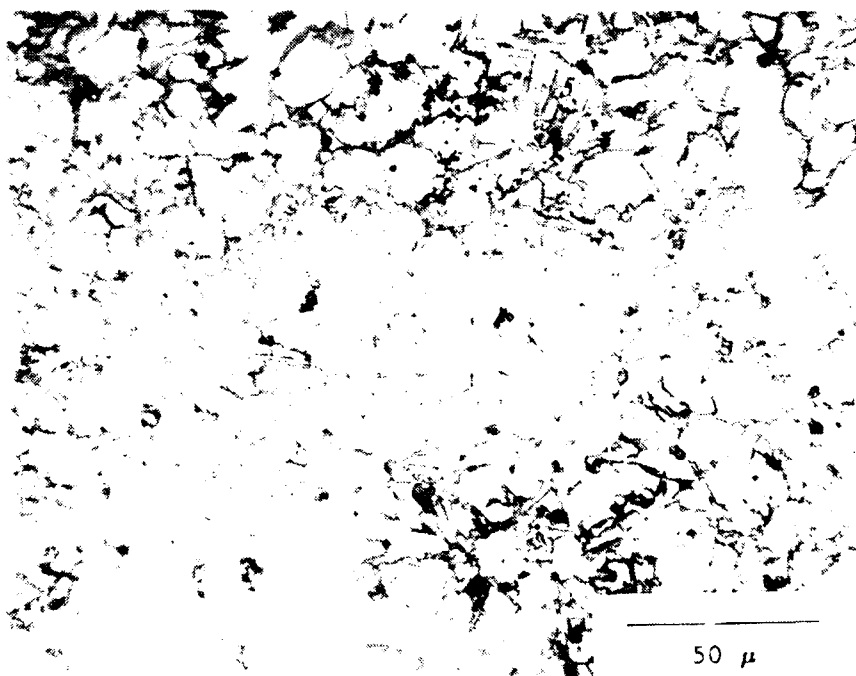
(b) The circumferential bulk area

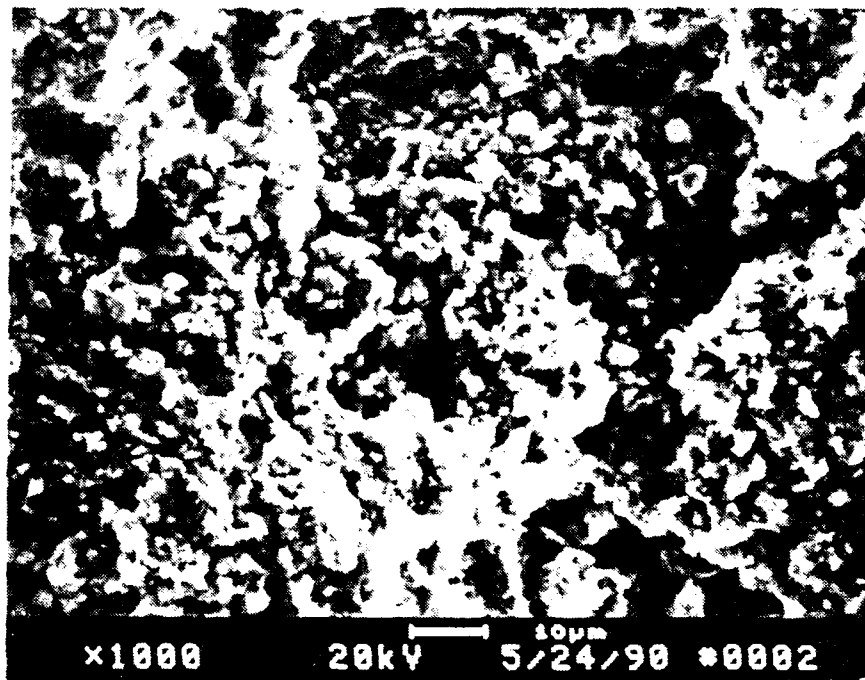Figure 6. The cast microstructure of the fuse holder.

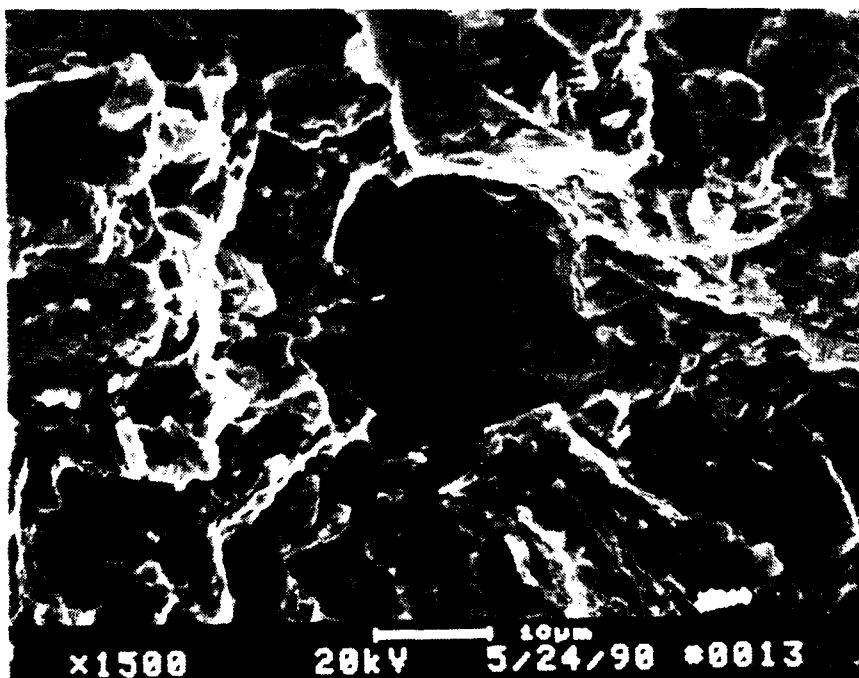Figure 7. A typical fracture surface showing ductile matrix with cracked brittle particles.

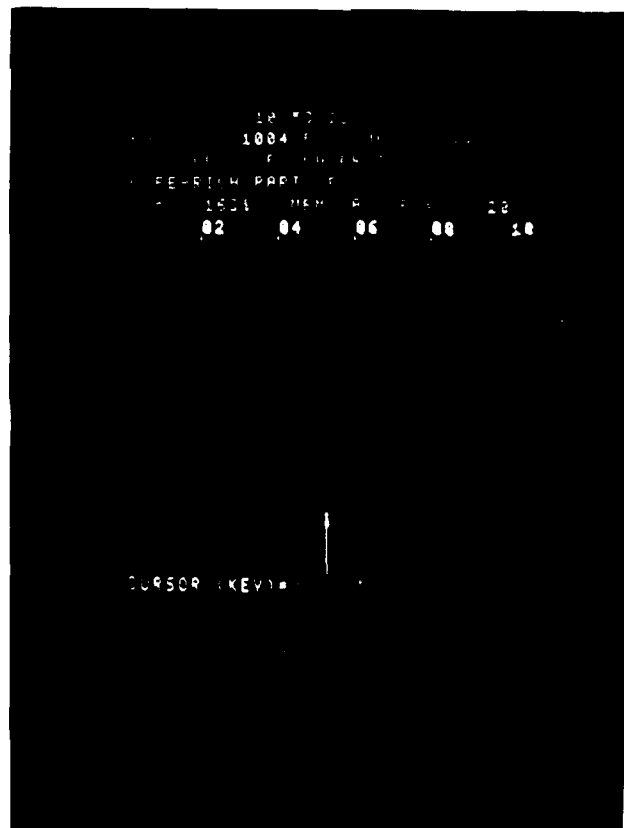Figure 8. A fracture cavity caused by cracking of an Fe-rich particle.
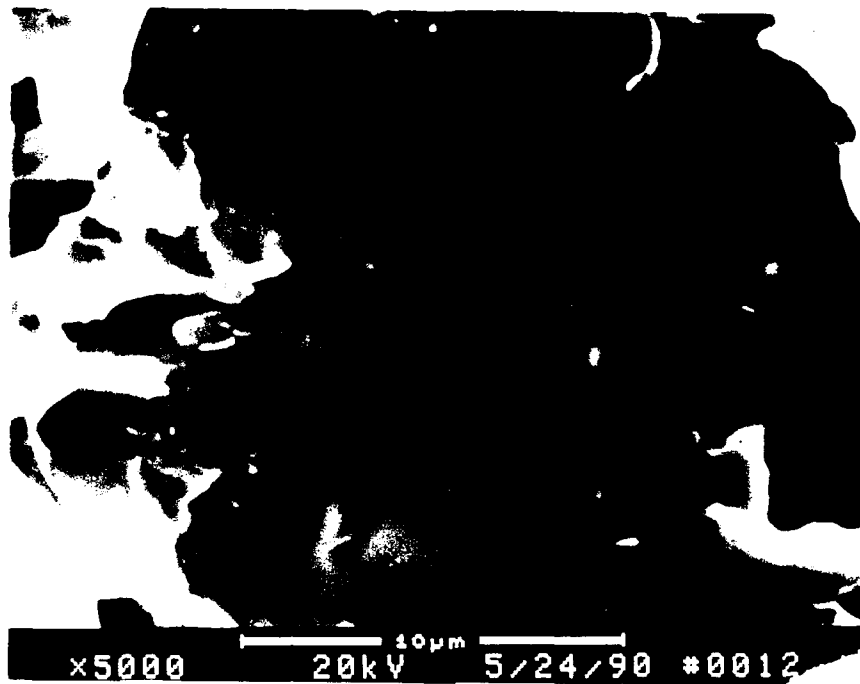
10

Figure 9. A close-up examination of the fracture cavity in Figure 8 with the EDS spectra.
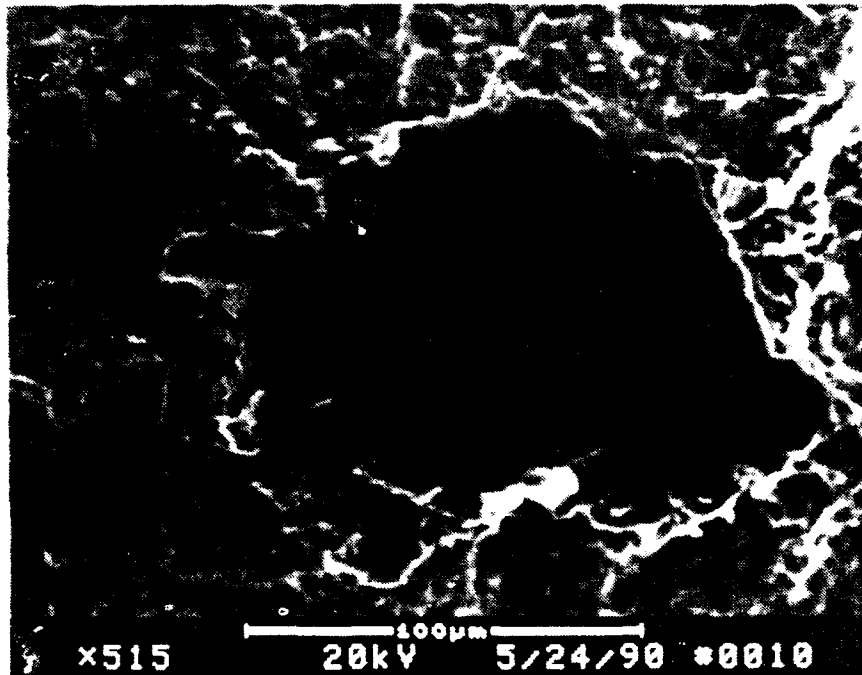
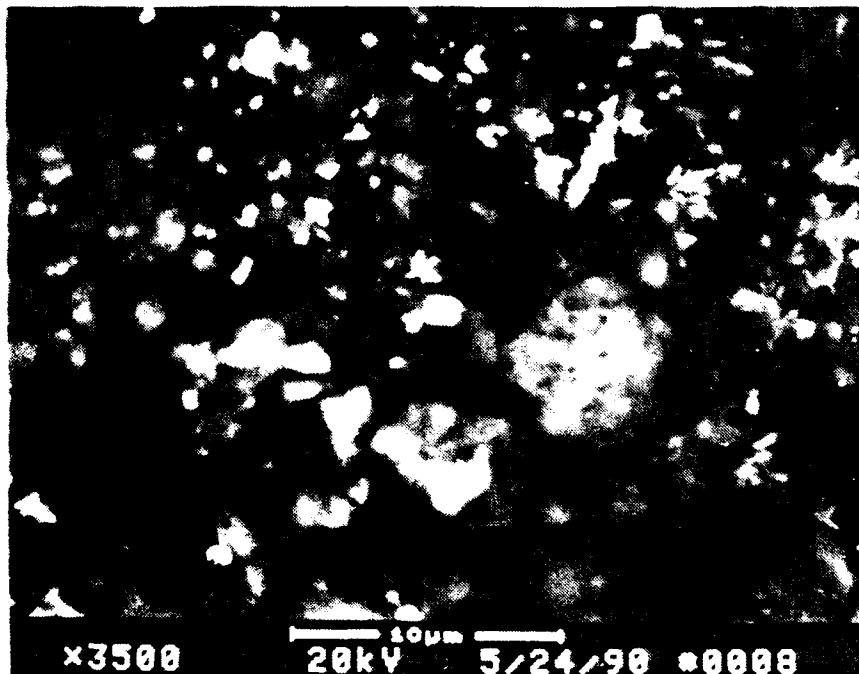Figure 10. A residual aluminum particle observed on the fracture surface.

Figure 11. Foreign inclusions and particles observed on the fracture surface.
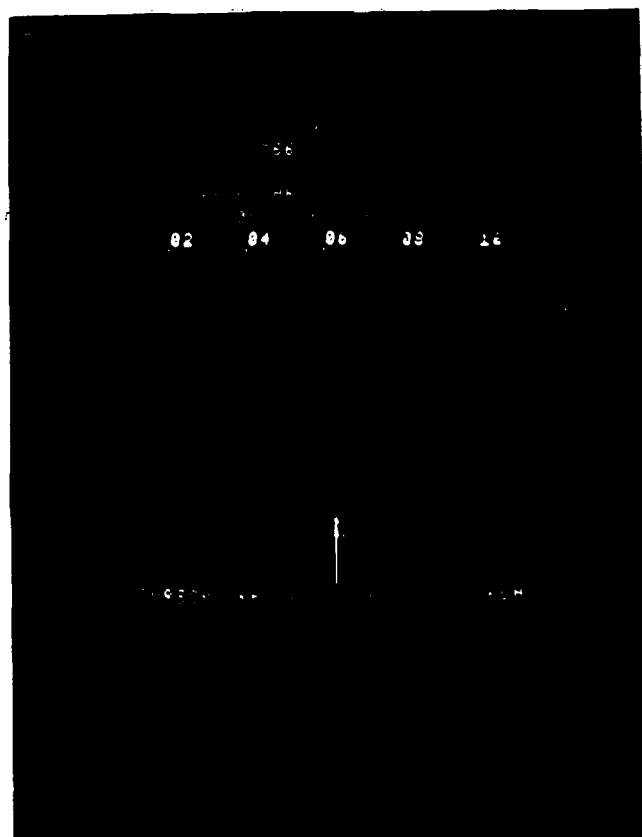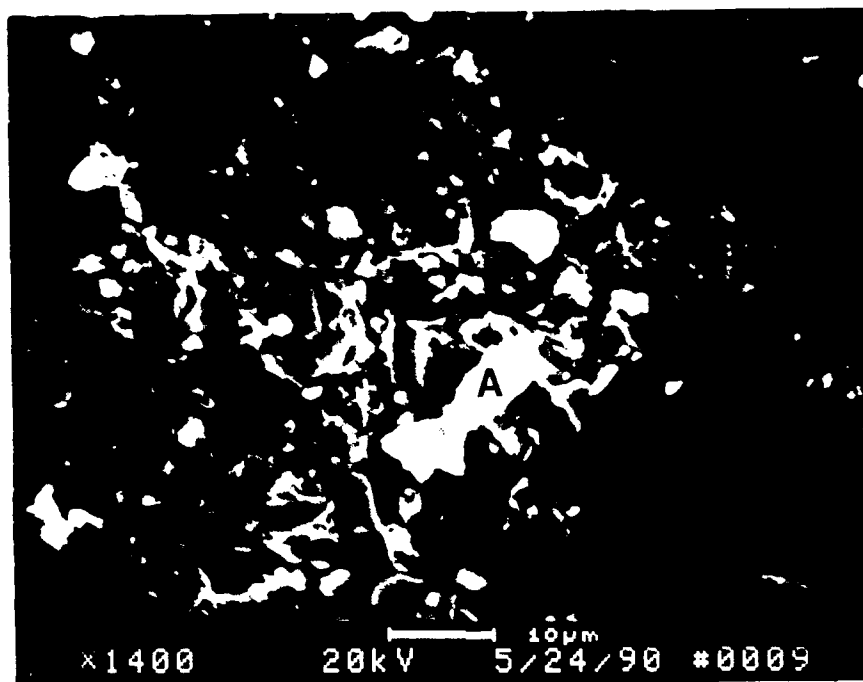
12

Figure 12. Pb-rich particle, A, observed on the fracture surface.

disc area has a higher average microhardness value than the circumferential bulk area as a result of its finer grained microstructures as shown in Figure 6. The population standard deviation σ_n is defined by the following equation:

$$\sigma_n = \sqrt{\frac{\sum x^2 - \frac{(\sum x)^2}{n}}{n}}$$

(1)

where x = individual microhardness value and n = number of tests. The relatively large population standard deviation for the hardness values measured for each sampling region is a consequence of the heterogeneity of microstructure and is more pronounced in the thicker section. A few "softer" spots resulting from the inclusion particles (i.e. Al or Pb, etc.) were also observed. However, any unusually low hardness values (< 51.0 Knoop) have been excluded from the calculation of the average microhardness values to reflect the "true" property of the matrix material.

Density and Porosity Evaluation

Limited porosity was observed during metallographic analysis. Image analysis was also conducted with the Buehler Omnimet II system, but it proved difficult and time consuming to distinguish porosity from second phase inclusions in the cast structure. The results as shown in Appendix II therefore probably err on the conservative side, i.e., the true porosity percentage is less than the data indicates. An analysis of 10 different fields shows that the average porosity is less than 4.6% in the thick section area and less than 1.6% in the thin section area. The theoretical density of 380 aluminum alloy is 2.74 g/cm^3 (0.098 lb/in^3) (2). However, the three measurements of the density averaged about 2.54 g/cm^3 indicating a maximum porosity less than 7%.

Process Evaluation

As described in the Metals Handbook, "Die casting is especially suited to productions of large quantities of relatively small parts. With die casting it is possible to maintain close tolerances and produce good surface finishes; aluminum alloys can be die cast to a basic linear tolerance of ± 4 mm/m (± 4 mils/inch) and commonly have finishes as fine as 1.3 µm (50 µinch)."(3). The center-cup area of the fuse holder has a specified thickness of 0.015+0.005 inch. This section has a measured thickness of 0.010 inch, which is well below the minimum required. It is clear that improvements in tolerances for this fuse holder are in order. "Die castings are best designed with a uniform wall thickness. The minimum practical wall thickness for aluminum alloy die casting is dependent on product size. Small parts can be cast as thin as 1.0 mm (0.04 inch),"(3) which is about 2.7 times thicker than the thinnest section of the center-cup area.

Air entrapment and shrinkage during the die casting process may result in porosity, and surface finishing cuts should be limited to 0.1 mm (0.040 inch) to avoid exposing it.(3) Several casting cavities were observed by optical microscopy.

The fuse holder is made of 380 aluminum alloy which is frequently used for such die casting applications. Approximately 85% of aluminum alloy die castings are produced with aluminum-silicon-copper alloys (alloy 380 and its several modifications). Since this family of alloys provides a good combination of cost, strength and corrosion resistance, together with the high fluidity and freedom from hot shortness that are required for easy casting (3), this alloy selection appears to be consistent with industry practice..

---

[3]   *ASM Metals Handbook*, p.143, v.2, 9th ed., Metals Park, Ohio, 1979.

STRESS ANALYSIS

Formulas

Based on our metallurgical analysis that the material was basically sound and the locations of the cracks observed, we concluded that these cracks were caused by mechanical stresses exceeding design values rather than by substandard material strength. The complex part geometry has limited the degree of accuracy for any quantitative stress analysis. Two mathematical formulas (4) were employed for analysis based on certain approximations and assumptions with regard to material properties, geometric complexity and boundary conditions. It is also often very difficult to decide whether a plate should be considered as freely supported or fixed, whether a load should be assumed uniformly or otherwise distributed. The simulated configuration for the current study is presented in Figure 13. The center-disc was approximated as a flat plate of average thickness with a firmly fixed edge. The load is assumed to be uniformly distributed. The maximum bending stress and deflection can then be calculated by the following equations:

$$\sigma = k\frac{wr^2}{t^2} \qquad (2)$$

$$y = k_1\frac{wr^4}{Et^3} \qquad (3)$$

where,

|		
σ	=	maximum bending stress
k	=	stress coefficient, 1.24
k_1	=	deflection coefficient, 0.696
w	=	uniform loading stress
r	=	disc radius
t	=	disc thickness
y	=	maximum deflection
E	=	Young's modulus

The above formulas apply primarily to symmetrically loaded plates of constant thickness, in which flexure stresses predominate. In this mathematical analysis, allowance for stress redistribution due to slight local yielding is not considered. Since this yielding, especially in ductile materials, is beneficial, the formulas generally err on the side of safety.(4)

Calculation and Analysis

Using the material parameters of aluminum alloy 380 listed in the Materials Section and Equations (2) & (3) the maximum tolerable explosive pressure can be calculated. The results are tabulated in Table II. The data for wrought 6061-T6 aluminum alloy is also included for comparison purposes.

---

[4] Mark's *Standard Handbook for Mechanical Engineers*, T. Baumeister, Editor-in-Chief, E.A. Avallone and T. Baumeister III, associate editor, 8th ed., p.5-52, McGraw-Hill, NY, NY, 1978.

15 ±5°

.150-.010"

radius,
.01" max

.12-.01"

.075±.005"
(.070")

.015+.005"
(.010")
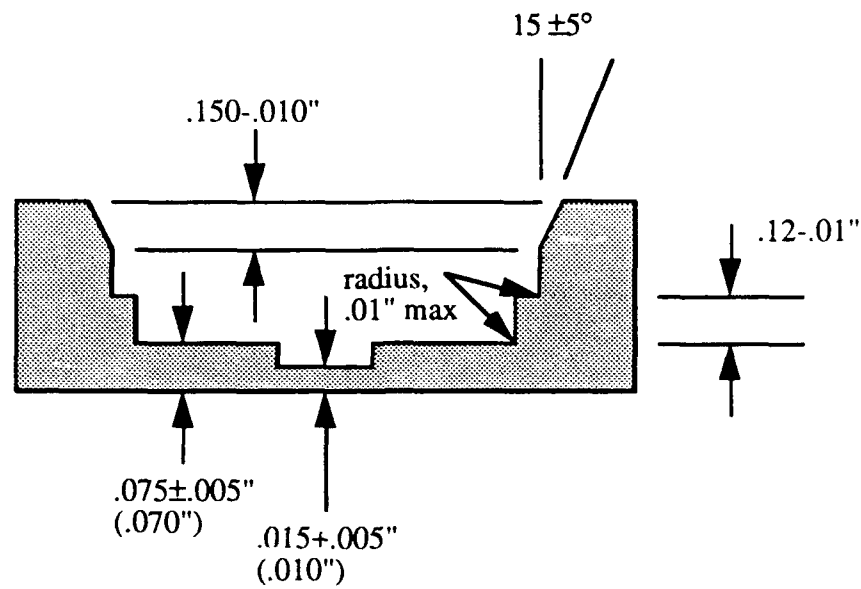
(a) True configuration with the measured dimensions in parentheses

w

r
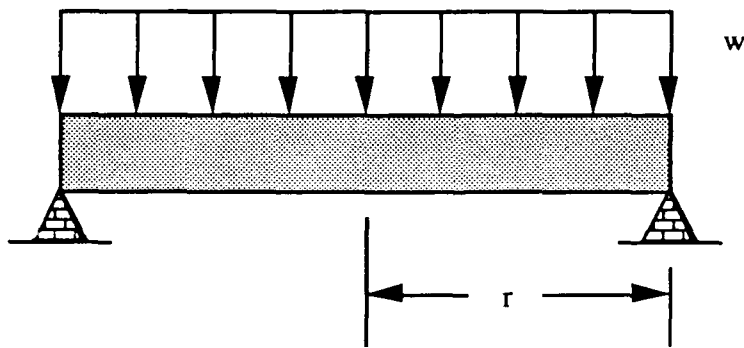
(b) Simulated configuration

Figure 13. Configurations for stress analysis

16

Table II. STRESS, EXPLOSIVE PRESSURE AND DEFLECTION BASED ON THE ORIGINAL DESIGN

Material/ Safety Factor	Yield Strength σ_y (ksi)	Disc Thickness t (in)	Disc Radius r (in)	Maximum Tolerable Explosive Pressure w (psi)	Maximum Deflection Calculated y (in)
Safety Factor = 1					
380 Al	23	0.075	0.6225	269.25	0.0085
6061 Al	35	0.075	0.6225	409.72	0.0130
Safety Factor = 2					
380 Al	11.5	0.075	0.6225	134.62	0.0042
6061 Al	17.5	0.075	0.6225	204.86	0.0065

The local explosive pressure resulting from fuse ignition is not expected to be uniformly distributed. The "true profile" of the local explosive pressure was not available. However, the values summarized in Table II provide a reasonable estimate for design purposes. Without considering the safety factor, i.e. safety factor = 1, the maximum tolerable explosive pressure is 269.25 psi for avoiding stressing the 380 aluminum alloy above its yield strength with a maximum deflection value of 0.0085 inch occurring in the center. Using a safety factor of 2, the maximum tolerable explosive pressure is 134.62 psi with a maximum deflection of 0.0042 inch in the center. Compared with the large measured deflection value in the center-cup area, 0.005 inch, the finding is alarming. The calculated explosive stress corresponding to this 0.005 inch deflection is 200 psi, which is larger than 134.62 psi; thus it is not surprising to find small su face cracks in the center-cup area.

It has been suggested in a new design that by increasing the thickness of the center-disc from 0.075 to 0.095 inch, the tolerable amount of explosive pressure and the resultant deflection can be improved as summarized in Table III.

For this newly recommended design the calculated deflection values in the center are 0.0067 and 0.0034 inch for safety factors 1 and 2, respectively. No experimental data are yet available to validate the "actual" deflection values occurred during the explosion. Nonetheless, the actual deflection values are expected to be larger than those calculated since the thin center-cup area is not considered in the calculation.

Stress Concentration

Stress concentration is another important factor contributing to crack initiation. An extensive quantitative analysis of the "exact" stress concentration effect is beyond the scope of the current study due to the variations of the geometry and the complexity of the mathematics. However, if we only consider the wall edge area where cracks occurred, and simulate the stress concentration behavior as that of the bending of a stepped flat bar with shoulder fillets, the stress concentration

Table III. STRESS, EXPLOSIVE PRESSURE AND DEFLECTION BASED ON THE NEWLY PROPOSED DESIGN

Material/ Safety Factor	Yield Strength σ_y (ksi)	Disc Thickness t (in)	Disc Radius r (in)	Maximum Tolerable Explosive Pressure w (psi)	Maximum Deflection Calculated y (in)
Safety Factor = 1					
380 Al	23	0.095	0.6225	431.99	0.0067
6061 Al	35	0.095	0.6225	657.38	0.0096
Safety Factor = 2					
380 Al	11.5	0.095	0.6225	216.00	0.0034
6061 Al	17.5	0.095	0.6225	328.69	0.0051

factor would be about 2 (5). By changing the fillet radius from 0.01 to 0.03 inch a reduction in the stress concentration factor to about 1.5 could be expected.

SUMMARY AND CONCLUSIONS

Metallurgical analysis shows that the material meets standard material requirements despite the heterogeneity in the cast microstructure that depends on section thickness and different local deformation resistance in the fuse holder due to geometrical factors. There is still some room for improvement in process optimization; die cast porosity could be further reduced and some undesirable impurity inclusions should be eliminated. The inherent heterogeneity in microstructure is a consequence of the overall design geometry with sections of different thicknesses; this can only be reduced by a completely new design which might not be feasible or satisfy other criteria. Dimensional allowance is also a concern due to the relatively small center-cup area thickness. Other factors permitting, a thicker central section might be worth consideration in future production runs.

It is our conclusion that the cracks found in the fuse holder are a consequence of stress concentration resulting from the impulsive impact force during the explosive firing. A detailed finite element analysis of stress would be helpful for a better understanding of stress distribution, but it is beyond the scope of this report. We endorse the proposed new design wherein the thickness of the center-disc is increased from 0.075±0.005 to 0.095±0.005 inch, and the fillet radius is also increased from 0.01 to 0.03 inch. Without altering other dimensions, 0.095±0.005 inch would be the maximum allowed thickness value in the current design due to geometric restrictions. However, we are concerned about the thickness of the center-cup region with the measured value of 0.010 inch while 0.015+0.005 inch is specified in the drawing.

5   P. E. Peterson, *Stress Concentration Factor*, p.98, John Wiley, NY, NY, 1974.

ACKNOWLEDGEMENT

APPENDIX I. MICROHARDNESS TESTING DATA

Testing Area	Thin-Left	Thin-Right	Bulk-Left	Bulk-Right
Testing Point	Micro Knoop Hardness Value			
1	90.5	96.8	83.9	87.3
2	90.9	90.8	97.0	91.4
3	97.3	95.8	98.8	94.5
4	98.6	91.6	86.8	80.5
5	95.8	98.0	78.8	87.5
6	96.8	98.8	90.9	84.5
7	98.8	101	60.6	94.7
8	105	98.7	99.9	71.1
9	99.5	99.7	98.4	68.7
10	99.7	104	94.8	94.1
11	101	102	99.2	88.7
12	97.8	104	91.4	99.2
13	98.6	98.0	94.2	89.5
14	97.2	97.0	101	92.0
15	94.0	101	97.7	91.0
16	101	99.6	98.9	85.7
17	99.8	98.6	96.4	82.8
18	96.2	95.6	86.9	95.4
19	100	94.7	(51.0)	95.4
20	98.3	99.3	70.7	100
21	97.3	101	96.7	103
22	93.3	99.6	(53.5)	86.5
23	103	85.9	90.5	92.1
24	105	99.1	63.4	59.0
25	102	100	101	100
26	101	104	89.7	99.4
Minimum	90.5	85.9	60.6	59.0
Maximum	105	104	101	103
Average	98.4	98.3	90.3	89.0
Std. Dev.	3.6	4.1	11.2	10.1

( ) Invalid readings due to soft inclusions at the indentation

20
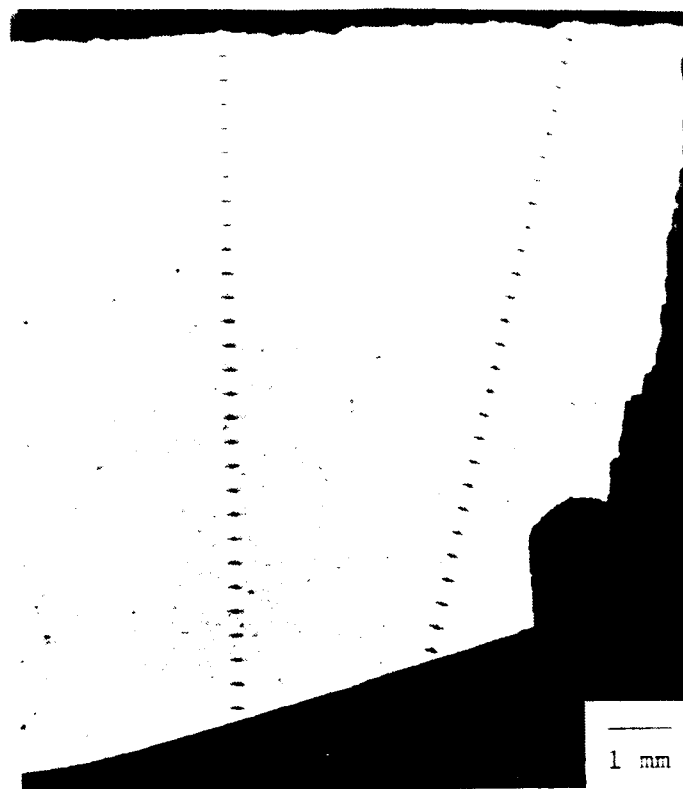
(a) The specimen cut from the thin center-disc area
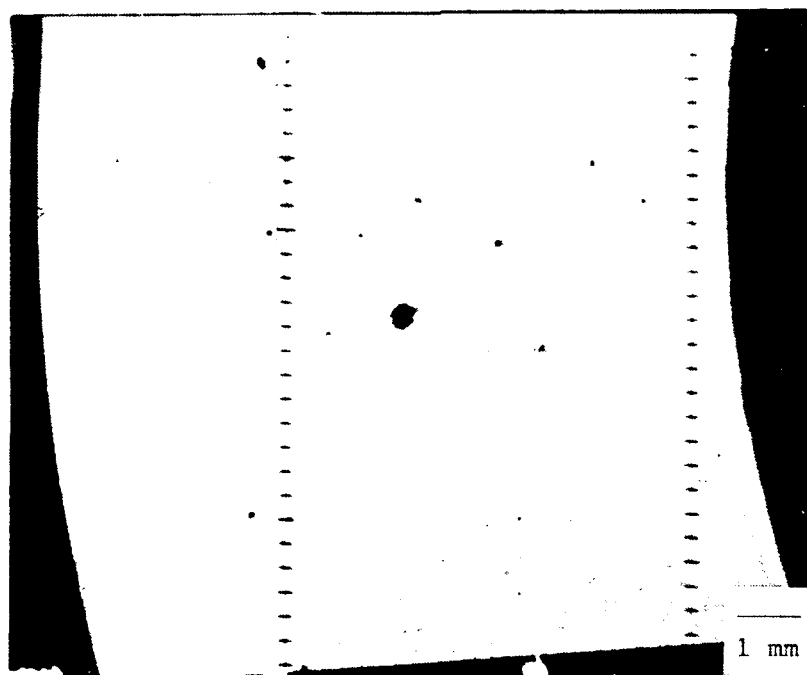
(b) The specimen cut from the circumferential bulk area

Figure IA. Photographs showing the microhardness testing locations
with a descending testing sequence from the left-top.

21

APPENDIX II. IMAGE ANALYSIS DATA

Field No	Porosity in Bulk Area (%)	Porosity in Thin Area (%)
1	4.0817	1.3590
2	5.2097	1.9122
3	4.5171	0.6701
4	4.4951	2.2402
5	4.5705	1.5272
6	4.6601	2.3073
7	4.0120	1.1699
8	3.8570	3.1015
9	6.0972	1.1725
10	4.3065	0.7136
Minimum	3.8570	0.6701
Maximum	6.0972	3.1015
Average	4.5807	1.6173
Standard Deviation	0.6570	0.7703

DISTRIBUTION LIST

No. of Copies	To

1 Office of the Under Secretary of Defense for Research and Engineering,
The Pentagon, Washington, DC 20301

Commander, U.S. Army Laboratory Command, 2800 Powder Mill Road, Adelphi,
MD 20783-1145
1 ATTN: AMSLC-IM-TL
1 AMSLC-CT

Commander, Defense Technical Information Center, Cameron Station, Building 5,
5010 Duke Street, Alexandria, VA 22304-6145
2 ATTN: DTIC-FDAC

1 MIAC/CINDAS, Purdue University, 2595 Yeager Road, West Lafayette,
IN 47905

Commander, Army Research Office, P.O. Box 12211, Research Triangle Park,
NC 27709-2211
1 ATTN: Information Processing Office

Commander, U.S. Army Materiel Command, 5001 Eisenhower Avenue,
Alexandria, VA 22333
1 ATTN: AMCSCI

Commander, U.S. Army Materiel Systems Analysis Activity,
Aberdeen Proving Ground, MD 21005
1 ATTN: AMXSY-MP, H. Cohen

Commander, U.S. Army Missile Command, Redstone Scientific Information Center,
Redstone Arsenal, AL 35898-5241
1 ATTN: AMSMI-RD-CS-R/Doc
1 AMSMI-RLM

Commander, U.S. Army Natick Research, Development and Engineering Center,
Natick, MA 01760-5010
1 ATTN: Technical Library

Commander, U.S. Army Satellite Communications Agency, Fort Monmouth, NJ 07703
1 ATTN: Technical Document Center

Commander, U.S. Army Tank-Automotive Command, Warren, MI 48397-5000
1 ATTN: AMSTA-ZSK
2 AMSTA-TSL, Technical Library

Commander, White Sands Missile Range, NM 88002
1 ATTN: STEWS-WS-VT

President, Airborne, Electronics and Special Warfare Board, Fort Bragg,
NC 28307
1 ATTN: Library

Director, U.S. Army Ballistic Research Laboratory, Aberdeen Proving Ground,
MD 21005
1 ATTN: SLCBR-TSB-S (STINFO)

Commander, Dugway Proving Ground, Dugway, UT 84022
1 ATTN: Technical Library, Technical Information Division

Commander, Harry Diamond Laboratories, 2800 Powder Mill Road, Adelphi, MD 20783
1 ATTN: Technical Information Office

Director, Benet Weapons Laboratory, LCWSL, USA AMCCOM, Watervliet, NY 12189
1 ATTN: AMSMC-LCB-TL
1 AMSMC-LCB-R
1 AMSMC-LCB-RM
1 AMSMC-LCB-RP

Commander, U.S. Army Foreign Science and Technology Center, 220 7th Street, N.E.,
Charlottesville, VA 22901-5396
3 ATTN: AIFRTC, Applied Technologies Branch, Gerald Schlesinger

No. of Copies	To
	Commander, U.S. Army Aeromedical Research Unit, P.O. Box 577, Fort Rucker, AL 36360
1	ATTN: Technical Library
	Commander, U.S. Army Aviation Systems Command, Aviation Research and Technology Activity, Aviation Applied Technology Directorate, Fort Eustis, VA 23604-5577
1	ATTN: SAVDL-E-MOS
	U.S. Army Aviation Training Library, Fort Rucker, AL 36360
1	ATTN: Building 5906-5907
	Commander, U.S. Army Agency for Aviation Safety, Fort Rucker, AL 36362
1	ATTN: Technical Library
	Commander, USACDC Air Defense Agency, Fort Bliss, TX 79916
1	ATTN: Technical Library
1	Clarke Engineer Scool Library, 3202 Nebraska Ave. North, Ft. Leonard Wood, MO 65473-5000
	Commander, U.S. Army Engineer Waterways Experiment Station, P. O. Box 631, Vicksburg, MS 39180
1	ATTN: Research Center Library
	Commandant, U.S. Army Quartermaster School, Fort Lee, VA 23801
1	ATTN: Quartermaster School Library
	Naval Research Laboratory, Washington, DC 20375
1	ATTN: Code 5830
2	Dr. G. R. Yoder - Code 6384
	Chief of Naval Research, Arlington, VA 22217
1	ATTN: Code 471
1	Edward J. Morrissey, WRDC/MLTE, Wright-Patterson Air Force, Base, OH 45433-6523
	Commander, U.S. Air Force Wright Research & Development Center, Wright-Patterson Air Force Base, OH 45433-6523
1	ATTN: WRDC/MLLP, M. Forney, Jr.
1	WRDC/MLBC, Mr. Stanley Schulman
	NASA - Marshall Space Flight Center, MSFC, AL 35812
1	ATTN: Mr. Paul Schuerer/EH01
	U.S. Department of Commerce, National Institute of Standards and Technology, Gaithersburg, MD 20899
1	ATTN: Stephen M. Hsu, Chief, Ceramics Division, Institute for Materials Science and Engineering
1	Committee on Marine Structures, Marine Board, National Research Council, 2101 Constitution Ave., N.W., Washington, DC 20418
1	Librarian, Materials Sciences Corporation, 930 Harvest Drive, Suite 300, Blue Bell, PA 19422
1	The Charles Stark Draper Laboratory, 68 Albany Street, Cambridge, MA 02139
	Wyman-Gordon Company, Worcester, MA 01601
1	ATTN: Technical Library
	Lockheed-Georgia Company, 86 South Cobb Drive, Marietta, GA 30063
1	ATTN: Materials and Processes Engineering Dept. 71-11, Zone 54
	General Dynamics, Convair Aerospace Division, P.O. Box 748, Fort Worth, TX 76101
1	ATTN: Mfg. Engineering Technical Library
	Director, U.S. Army Materials Technology Laboratory, Watertown, MA 02172-0001
2	ATTN: SLCMT-TML
3	Authors

U.S. Army Materials Technology Laboratory,
Watertown, Massachusetts 02172-0001
METALLURGICAL AND MECHANICAL ANALYSES OF A
FAILED FUSE HOLDER FROM THE XM264 ROCKET -
Wego Wang, John C. Beck, and Martin G. H. Wells

AD _____
UNCLASSIFIED
UNLIMITED DISTRIBUTION

Key Words

Aluminum alloys
Die casting
Radiography

Technical Report MTL TR 91-31, August 1991, 25 pp -
illus-tables

One aluminum fuse holder from the XM264 red phosphorus smoke rocket that failed during testing was analyzed to determine the cause of failure. Cracks were observed on both sides of the die cast fuse holder. Radiographic analysis was conducted to confirm the damage observed. All the dimensions of this failed fuse holder were found to be within the requirements specified in the part drawing, except the central cup. This region was 30% thinner than specified. Metallographic analysis indicated a mixed fine-grained and eutectic structure in the thin center-disc area and a large dendritic structure in the thick circumferential area. Fractographic examination of the fracture surface showed fracture initiating at large brittle impurity-rich particles. A stress analysis concluded that failure occurred as a result of insufficient material thickness in the central cup region and from stress concentration around the wall edge. Suggestions for a new design with thicker central sections were confirmed by U.S. Army Chemical Research, Development and Engineering Center at Aberdeen Proving Ground, Maryland.